Proceedings of the ASME 2018 5th Joint US-European Fluids Engineering Division Summer Conference
FEDSM2018
July 15-20, 2018, Montreal, Quebec, Canada

FEDSM2018-83223

ASSESSMENT OF CAVITATION MODELS IN THE PREDICTION OF CAVITATION IN NOZZLE FLOW

Dorien O. Villafranco, Huy K. Do, Sheryl M. Grace, Emily M. Ryan, R. Glynn Holt
Department of Mechanical Engineering
Boston University
Boston, Massachusetts 02215
Email: dvillafr@bu.edu

ABSTRACT

Cavitation inside fuel injector nozzles has been linked not only to erosion of the solid surface, but also to improved spray atomization. To quantify the effects of the resulting occurrences, the prediction of cavitation through computational modeling is vital. Homogeneous mixture methods (HMM) make use of a variety of cavitation sub-models such as those developed by Kunz, Merkle, and Schnerr-Sauer, to describe the phase change from liquid to vapor and vice-versa in the fluid system. The aforementioned cavitation models all have several free-tuning parameters which have been shown to affect the resulting prediction for vapor volume fraction.

The goal of the current work is to provide an assessment of the Kunz and Schnerr-Sauer cavitation models. Validation data have been obtained via experiments which employ both acoustic techniques (passive cavitation detection, or PCD) and optical techniques (optical cavitation detection, or OCD). The experiments provide quantitative information on cavitation inception and qualitative information as to overall vapor fraction as a function of flow rate, and nozzle geometry. It is shown that inception is fairly well captured but the amount of vapor predicted is far too low. A sensitivity analysis on the tuning parameters in the cavitation models leads to some explainable trends, however, several parameter sweeps results in outlier predictions. Recommendations for their usability and suggestions for improvement are presented.

INTRODUCTION

Cavitation refers to the rapid growth and subsequent collapse of air bubbles in a liquid. This process of bubble formation is a result of pressure fluctuations in the fluid field. When the pressure in the liquid falls below a certain threshold, vapor and gas-filled nuclei can grow into bubbles [1]. If the bubbles are convected to regions of high pressure in the fluid system, they collapse, often resulting in the erosion of nearby solid surfaces [2]. Cavitation occurs in fuel injectors. A wide-range of pressures inside the nozzle result in cavitation in this system.

It is known that cavitation inside the nozzle of the fuel injector causes the atomized spray to contain smaller droplets and results in a wider spray angle [3]. Smaller droplets in the spray and wider spray angles have been linked to significant reductions in emissions from engines [3,4]. Cavitation is also the major reason for fuel injector damage as collapsing bubbles erode the solid surface of the injector [2].

Various numerical models have been developed with the aim of simulating cavitating flows. The most widely used class is the homogeneous mixture method (HMM) model [2, 5–13]. HMM models provide solutions for flow of two immiscible incompressible fluids under isothermal conditions with the ability to model phase change between these fluids. These are further classified as being of the barotropic equation type or the transport equation model (TEM) type. The former makes use of an equation of state to close the relationship between pressure and density and has been most heavily utilized by Schmidt and his collaborators [14–19]. The equation of state most commonly employed, is written as $\frac{D\rho_m}{Dt} = \frac{1}{c^2}\frac{DP}{Dt}$ where ρ_m defines the density of the mix-

ture associated with the two fluids and c is the fluid sound speed. This is barotropic with continuously parallel gradients of density and pressure [2]. Experimental findings exhibit the importance of vorticity production in cavitating systems [20] which require a non-barotropic relationship between pressure and density [21]. Thus, the TEM seems more physical and is used in this work.

TEMs utilize an incompressible two-phase Navier-Stokes solver with mass transfer coupled into the equations which allows for the simulation of cavitation. Several sub-models which describe the phase change phenomenon exist, for example, those developed by Kunz [22], Merkle [23] and Schnerr-Sauer [24]. The implementation of all these sub-models rely on the specification of several empirical parameters which must be tuned for the particular flow being considered.

The aim of this work is to assess the ability of these cavitation models to predict cavitation in nozzle flow. Furthermore, a sensitivity analysis of the various empirical parameters on the cavitation prediction is conducted. The analysis is carried out by comparing results from computational results obtained using OpenFOAM to acoustic and optical cavitation detection methods of flow in a cylindrical nozzle. Pressure fluctuations in the nozzle result in transient cavitation in the system.

NUMERICAL MODELS

The incompressible unsteady RANS equations along with the transport equation model, presented below in Cartesian coordinates, were used to simulate cavitating flows. Body forces and heat transfer effects are assumed to be negligible in the problem being studied.

$$\frac{\partial \rho_m}{\partial t} + \nabla \cdot \left(\rho_m \mathbf{u}\right) = 0 \tag{1a}$$

$$\frac{\partial \rho_m \mathbf{u}}{\partial t} + \nabla \cdot \left(\rho_m \mathbf{u}\mathbf{u}\right) = \nabla P + \nabla \cdot \tau \tag{1b}$$

$$\frac{D}{Dt}\rho_v \alpha_v + \rho_v \alpha_v \nabla \cdot \left(\mathbf{u}\right) = R_{source} \tag{1c}$$

Here, $\mathbf{u}$ is the velocity of the mixture, P is the local pressure of the fluid, and τ is the deviatoric stress tensor. The mixture density ρ_m is defined as the weighted average between the density of the liquid (ρ_l) and the vapor (ρ_v) phases: $\rho_m = (1-\alpha_v)\rho_l + \alpha_v \rho_v$. Equation 1c shows the continuity equation for the vapor volume fraction defined as $\alpha_v = \frac{V_v}{V_{cell}}$.

The mass source term, R_{source}, on the right hand side of equation 1c is related to the phase transitions which occur. The term signifies the net rate between the processes of evaporation and condensation: $R_{source} = R_v + R_c$ where R_c models the condensation and R_v models the vaporization. The differences in the various cavitation models which use the TEM approach lie in the formulation of the source term.

In OpenFOAM version 4.1 [25], the simulation software of choice, the above equations are modeled in the solver interPhaseChangeFoam. This is a HMM solver which makes use of the Volume of Fluid (VOF) technique to discern the fluid state occupying computational cells in the domain. There are three cavitation models implemented into the interPhaseChangeFoam solver in OpenFOAM, namely those by Kunz, Merkle, and Schnerr-Sauer. This study will focus on the Kunz and Schnerr-Sauer cavitation models as they are the most common models seen in the nozzle cavitation literature.

Cavitation Models

Kunz

Kunz's cavitation model splits the phase change processes into two separate terms, and makes a determination as to which process is occurring by comparing local pressure to the vapor pressure of the liquid. The process of evaporation is modeled such that the evaporation rate is proportional to the liquid volume fraction and the difference between the vapor pressure and local pressure. Condensation is modeled using a simplified version of the Ginzburg-Landau potential [22].

$$\dot{m}^- = \frac{C_v \rho_v \alpha_l min[0, p - p_v]}{\left(0.5 \rho_l U_\infty^2\right) t_\infty} \tag{2a}$$

$$\dot{m}^+ = \frac{C_c \rho_v (\alpha_l)^2 (1-\alpha_l)}{t_\infty} \tag{2b}$$

The free parameters which appear in the model include C_c and C_v which respectively govern the rates of condensation and vaporization, a reference flow velocity, U_∞, and a reference time t_∞. α_l refers to the liquid volume fraction, and maintains the relationship of $\alpha_l = 1 - \alpha_v$ with the vapor volume fraction. In OpenFOAM [25], the default value for the empirical constants C_c and C_v is 100 as also noted in the original formulation by Kunz [22]. Bicer [26] has shown that changes in these constants result in significant changes in the vapor volume fraction predicted from the calculation.

Schnerr-Sauer

The Schnerr-Sauer model is argued to be one of the more sophisticated cavitation models since it draws its formulation from bubble dynamics. In this model, the vapor volume fraction is defined as:

$$\alpha_v = \frac{V_v}{V_{cell}} = \frac{N_{bubbles} \cdot \frac{4}{3}\pi R^3}{V_v + V_l} = \frac{n_0 V_l \cdot \frac{4}{3}\pi R^3}{n_0 V_l \cdot \frac{4}{3}\pi R^3 + V_l} = \frac{n_0 \cdot \frac{4}{3}\pi R^3}{1 + n_0 \cdot \frac{4}{3}\pi R^3} \tag{3}$$

where V_{cell} is the volume of the computational cell, V_v and V_l are the volumes occupied by vapor and liquid respectively, $N_{bubbles}$ is the number of bubbles in the computational cell, n_0 is defined

as the bubble concentration per unit volume of pure liquid, and R is the bubble radius. The model assumes that initial nuclei of the same size are homogeneously distributed throughout the computational domain. The well known Rayleigh-Plesset (RP) equation governs the growth and collapse of bubbles in a free field.

$$\underbrace{R\frac{d^2R}{dt^2}}+\frac{3}{2}\left(\frac{dR}{dt}\right)^2=\frac{p(R)-p_\infty}{\rho_l}-\underbrace{\frac{2\sigma}{\rho_l R}}-\underbrace{4\frac{\mu}{\rho_l R}\frac{dR}{dt}} \tag{4}$$

Schnerr-Sauer makes the argument that if the pressure is sufficiently low and the pressure difference described by p(R) - p_∞ is large, the under-braced terms from the RP equation may be ignored. p(R) is the liquid pressure inside at the bubble boundary usually set to the vapor pressure p_{vap}, and p_∞ is the ambient pressure. Therefore, the growth of the nuclei in the computational domain can be approximated as

$$\dot{R}=\sqrt{\frac{2}{3}\frac{p(R)-p_\infty}{\rho_l}} \tag{5}$$

This term was also noted by Holland and Apfel [27] as the driving term for bubble growth in predicting acoustic cavitation, but their criterion for cavitation was relating local pressure to the Blake Pressure and not the saturated vapor pressure of the liquid. Finally, Schnerr-Sauer [24] gives the forcing term in the transport equation (1c) as:

$$R_{source}=C_{c|v}\frac{\rho_l\rho_v}{\rho_m}\alpha_v(1-\alpha_v)sgn(p-p_{vap})\frac{3}{R}\sqrt{\frac{2}{3}\frac{|p-p_{vap}|}{\rho_l}} \tag{6}$$

COMPUTATIONAL SPECIFICATIONS

In order to compare the predictive capabilities of each cavitation model, and the sensitivity of the prediction to input model parameters, cavitation in a simple step nozzle was studied. Shown below in Figure 1 and 2 is the schematic and computational domain of the nozzle respectively. The step nozzle has a cylindrical inlet with an opening of 28.98 mm, and then flows into a square nozzle of 2.50 mm opening and 6.34 mm length.

The mesh used in the computational study was created using the SALOME mesh generator, and converted for use in OpenFOAM using the *ideasUnvToMesh* utility. It is an unstructured mesh composed of tetrahedral cells refined near the square nozzle for precise prediction in the cavitating region. The domain consists of 152,000 cells. Mesh properties such as cell skewness, aspect ratio, and non-orthogonality were ensured to be suitable

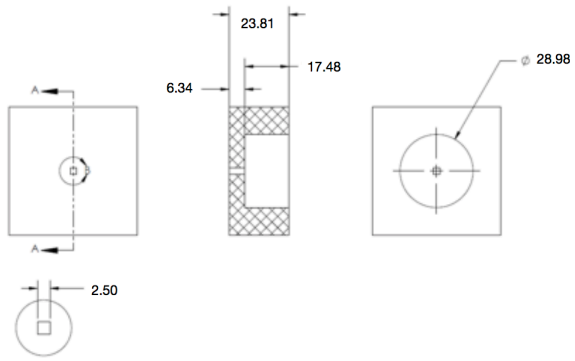

FIGURE 1. SCHEMATIC OF NOZZLE

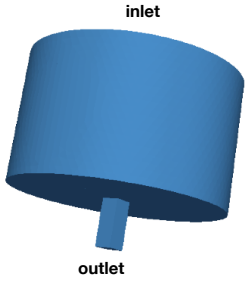

FIGURE 2. COMPUTATIONAL DOMAIN OF NOZZLE

by using the *checkMesh* utility in OpenFOAM. The simulations were run for a total time of 50 ms with time-steps of 1x10^{-10}s allowing for adjustable time-steps to maintain a Courant number of less than 0.1. Densities of 1000 kg/m^3 and 1.2 kg/m^3 and kinematic viscosities of 1.0x10$^{-6}m^3/s$ and 15.0x10$^{-6}m^3/s$ were respectively used for the liquid and vapor phases of the simulation. For time integration, a second order Euler scheme employing backward difference was used while the spatial discretization was done using second-order upwind Gauss schemes. A k-ε turbulence model was used with default wall functions for turbulent quantities k, ε and v_t. For the solution of pressure, the iterative PIMPLE algorithm is used with 2 iterations allowed for non-orthogonal corrections. Simulations were run using MPI parallelization built into OpenFOAM. The calculations were done using resources on Boston University's Shared Computing Cluster (BU SCC). Each calculation was parallelized to use 8 cores with the average CPU time for each run being about 20 CPU hours.

EXPERIMENTAL SETUP

To serve as a benchmark to the numerical calculations conducted in OpenFOAM, the nozzle described above was created

using acrylic to allow for experimental cavitation studies. A schematic of the experimental setup is shown in Figure 3. A 3 gallon tank served as the reservoir in which the water volume remained constant and was recirculated. The nozzle was back-lit using a stroboscopic back-light and optically imaged using a Basler acA1920-25um CMOS camera. Optical settings of the camera such as exposure, interframe, gain, dynamic range, ROI and binning were set using camera software. The camera was interfaced with the computer using a USB3 serial interface.

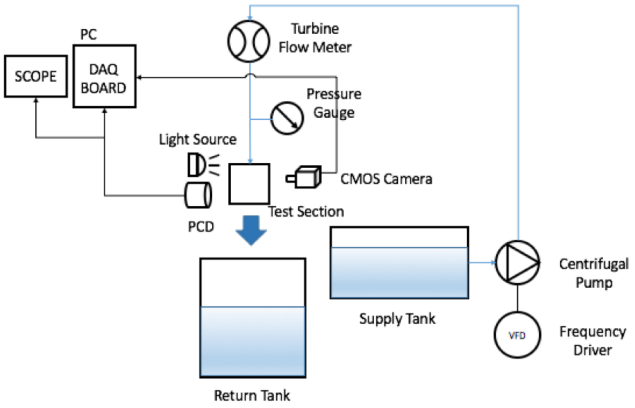

FIGURE 3. SCHEMATIC OF EXPERIMENTAL SETUP

For passive acoustic sensing, two unfocused single piezo-ceramic element Olympus transducers were used. These transducers had center frequencies of 5 and 10 MHz and the quality factor was about 10 to augment the sensitivity to transient events. Signals from the transducer were acquired using a Lecroy DSO which was controlled through a GPIB interface which allowed transfer of signals to the computer. No filtering or amplification of the signal was employed. To control the input flow, a March centrifugal pump with Variac variable voltage input was used. Shown in Table 1 are the various flow rates that were used.

A water sample of 60 ml used in this experiment was tested to obtain a number weighted distribution of the particle sizes inside the water. It was found that particles ranged from $0.5\mu m$ to 400 μm in diameter with an average nuclei diameter of $0.7\mu m$. Since the models, to date, are unable to have a distribution of nuclei sizes specified, the average nuclei size, and total vapor volume was used to calculate a concentration to be used in the HMM. The total vapor volume in the tested liquid was $9.07\text{x}10^{-9}m^3$. To account for this volume, $4.22\text{x}10^7$ nuclei of $0.7\mu m$ diameter are needed. This resulted in a concentration of $7.0\text{x}10^6$ nuclei/m^3. The average nuclei diameter along with the calculated concentration were used in the simulations.

TABLE 1. MEASURED FLOW RATE AND VELOCITIES FOR CAVITATION EXPERIMENTS

Case	Flow Rate (lpm)	Inlet Velocity (m/s)	Cavitation
1	2.68	0.068	No
2	5.60	0.140	No
3	8.23	0.210	Yes
4	10.06	0.250	Yes
5	12.26	0.310	Yes
6	14.31	0.360	Yes

RESULTS

In the experiments, OCD and PCD were used to determine cavitation inception. The nozzle was subject to several flow rates as described in Table 1. Optical imaging allowed for the visualization of vapor inside the nozzle. Figure 4 compared images obtained from OCD of a non-cavitating case and a cavitating case. The dark clouds near the walls of the nozzle are a manifestation of vapor cavities having formed. In terms of passive cavitation detection, a transducer was used to register voltages from acoustic excitations in the nozzle. Figure 5 shows a clear change in voltage between the non-cavitating case and the cavitating case. The change in voltage is due to the impulsive excitation of bubbles collapsing through the fluid. It was found that increasing the flow-rate past 8.23 lpm resulted in the development of vapor cavities in the fluid flow. This was confirmed by both detection techniques.

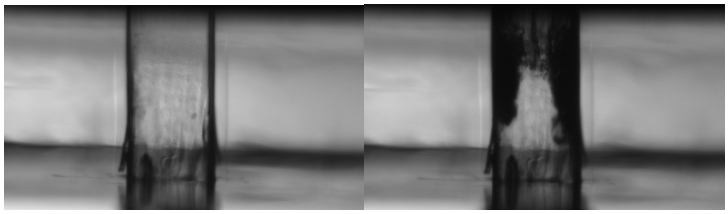

(a) Flow Rate = 2.68 lpm (b) Flow Rate = 8.23 lpm

FIGURE 4. OPTICAL CAVITATION DETECTION

The results of the OCD and PCD methods are summarized in Figure 6. Mean brightness, a marker of OCD, and Voltage, a marker of PCD, are shown as functions of outlet nozzle velocity. As can be seen in the figure, increases in velocity result in increases in both mean brightness and voltage. It can be discerned that the system shows definite signs of cavitation after

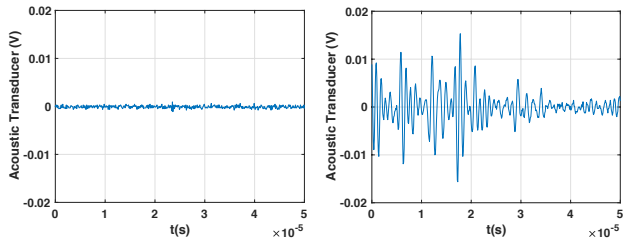

(a) Before Cavitation Detection (b) After Cavitation Detection

FIGURE 5. PASSIVE CAVITATION DETECTION

the outlet velocity reaches a value of 27 m/s. This corresponds to an inlet flow rate of 8.23 lpm (case 3) in the studied cases. It is interesting to note that the PCD starts to show a decrease in recorded voltage after the outlet velocity is further increased. This is due to the nozzle experiencing hydraulic flip. This is a phenomenon in which cavitation vanishes due to downstream air at the outlet moving upstream into the nozzle [28]. Optically, air is still visible as indicated in steady rise in mean brightness in the hydraulic flip regime. Cavitation, however, which refers to the growth and collapse of air bubbles, is lessened. Being able to capture the reduction in cavitation due to hydraulic flip highlights one of the advantages of PCD.

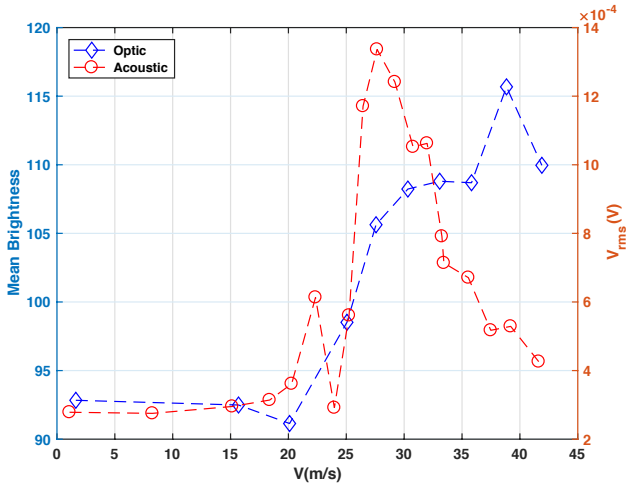

FIGURE 6. OPTICAL AND PASSIVE CAVITATION DETECTION

The validation for this study came from nozzle flow experiments using tap water as described above. The experiments provide quantitative information for cavitation onset and qualitative for volume fraction under cavitating conditions. To assess the ability of the cavitation models to predict varying levels of cavitation, simulations were run for the same inlet velocities and nozzle configurations as the experiment. The default constants for condensation (C_c) and vaporization (C_v) of 1 for the Schnerr-Sauer model were used along with the calculated parameters for n_o and d_{Nuc} of 7.0x10^{11} nuclei/m^3 and 0.7μm respectively. Outlet velocities and vapor volume fraction fields obtained from the simulations were compared to experimental results. Table 2 shows the comparison between the predicted outlet velocities from the multiphase simulations and those obtained from experimental measurements. As shown, the simulations do well in predicting the outflow velocities as dictated by the experiments.

TABLE 2. COMPARISON OF OUTLET VELOCITIES FROM EXPERIMENTS AND SIMULATIONS

Case	Inlet Velocity (m/s)	Outlet Velocity [Exp.] (m/s)	Outlet Velocity [Sim.] (m/s)
1	0.068	9.10	6.95
2	0.140	19.01	18.27
3	0.210	27.93	24.80
4	0.250	34.16	34.81
5	0.310	41.63	39.87
6	0.360	48.59	46.25

Images obtained from the experiment show a qualitative comparison to the simulations. Cavitation inception seems to be captured to some degree. Figure 7 shows no cavitation before the threshold flow rate of 8.23 lpm and cavitation after, however, it is clear that the simulations do not accurately predict the extent of the cavitating region for the cases being studied. Cavitation is severely under predicted in the simulations. It should be noted that the simulations, though transient, do not see huge variations in the regions where cavitation occurs. It is true that in the experiments, exposure time may be a factor. The settings on the camera would record a dark region even if the area is only occupied by a cavity for some fraction of the exposure time. In addition, a cavity of a finite size will be advected some finite length during the exposure time resulting in the experimental image being dark for a larger region than the cavity actually occupied. Nonetheless, current simulations, even when compared over a length of time do not show significant differences in the regions where cavitation is predicted.

The Schnerr-Sauer cavitation model employs a rather simplistic inception criterion by simply comparing the local

pressure in the liquid to the saturated vapor pressure of the liquid, and only allows for nuclei of a single size to be dispersed in the system. These model constraints may be the reason for the discrepancy between the experimental results and the simulations in terms of overall vapor production. The current sample of water used in the experiments has nuclei ranging from $0.5\mu m$ to $400\mu m$. While the larger nuclei are indeed less in number, they will cavitate at about the saturated vapor pressure according to the Blake Threshold [1] while the smaller nuclei require greater liquid tension to cavitate. This could be why a greater amount of cavitation is visible in the experiments than those seen in the simulations. Alternatively, enough nuclei may not be included in the model because wall sites here have been completely neglected. These hypotheses are explored in the following section. Moreover, the effect of wall nucleation is not considered in these models. Surface roughness may serve as nucleation sites for cavitation to occur [1]. The size and number of nuclei used in the simulations was based on the average size in the water from the experiment and the number needed to obtain the overall volume fraction in the water. No potential wall nuclei have been included.

Sensitivity Analysis

Schnerr-Sauer

A parameter sweep of the Schnerr-Sauer cavitation model is now considered. Simulations were completed using different values for C_c, C_v, n_o and d_{Nuc} as specified in table 3. Given that the calculated concentration of $7.0\text{x}10^{11}$ was unable to provide volume fractions comparable to the experiment, larger values for concentration were investigated spanning a total of four orders of magnitude. In the same fashion, the initial diameter of the nuclei was increased with 6 total nuclei sizes being studied ranging from $0.7\mu m$ to $20\mu m$. To quantify the effect of the variation of input parameters, an iso-volume of vapor was calculated for cells which had vapor fractions of 0.5 or less at the end of each simulation. It should be noted that the calculation of this volume is at a single time-frame in the simulation. All simulations in the parameter sweep had an inlet velocity specification of 0.36 m/s which corresponded to Case 6 in the list of experiments.

Figure 8 shows the relationship between nuclei diameter, d_{Nuc} and vapor volume for various nuclei concentrations. There exists the representative trends of larger nuclei producing more vapor for a given concentration, and larger concentrations producing more vapor for a given nuclei size. There exists though a deviation from the trend after a certain threshold for both nuclei size and concentration. It can be seen from the figure that for a nuclei concentration of $7.0\text{x}10^{13}$, the vapor volume at the end of the simulation decreases if the initial nuclei diameter is increased past $7\mu m$. This happens just after $1\mu m$ for a concentration of $7.0\text{x}10^{14}$. The decrease in vapor production is due to the fact that larger nuclei sizes at large concentration

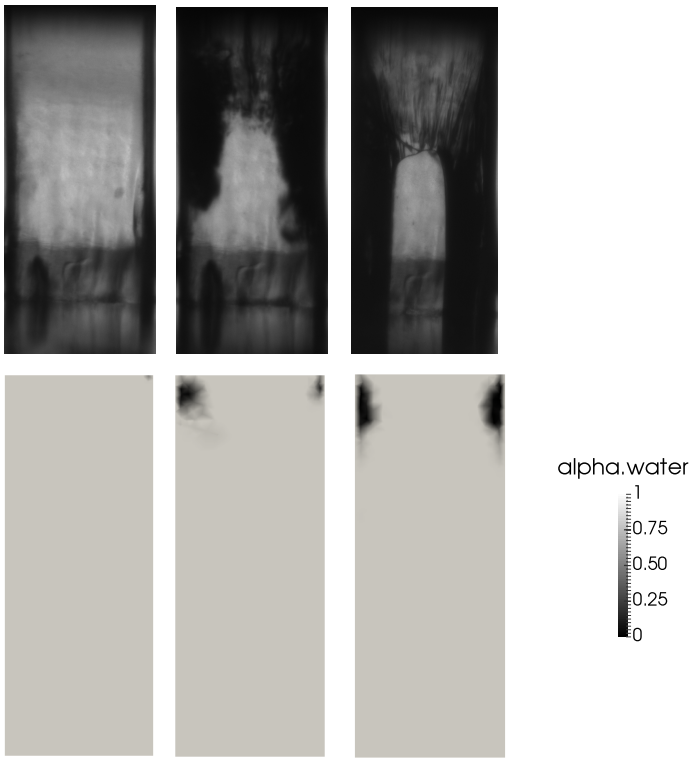

(a) 2.68 lpm (b) 8.23 lpm (c) 14.31 lpm

FIGURE 7. CAVITATION SIMULATIONS COMPARED TO EXPERIMENT

TABLE 3. PARAMETERS USED IN SENSITIVITY STUDY FOR SCHNERR-SAUER MODEL

C_c, C_v	n_o (#/m^3)	$dNuc$ (μm)					
1,1	$7.0\text{x}10^{+11}$	0.7	1.0	3.0	7.0	10.0	20.0
	$7.0\text{x}10^{+12}$	0.7	1.0	3.0	7.0	10.0	20.0
	$7.0\text{x}10^{+13}$	0.7	1.0	3.0	7.0	10.0	20.0
	$7.0\text{x}10^{+14}$	0.7	1.0	3.0	7.0	10.0	20.0
100,100	$1.0\text{x}10^{+11}$	0.7	1.0	3.0	7.0	10.0	20.0
	$1.0\text{x}10^{+12}$	0.7	1.0	3.0	7.0	10.0	20.0
	$1.0\text{x}10^{+13}$	0.7	1.0	3.0	7.0	10.0	20.0
	$7.0\text{x}10^{+14}$	0.7	1.0	3.0	7.0	10.0	20.0

initializes the simulation with an amount of vapor that is on the scale of the volume of the nozzle itself. The hydrodynamics

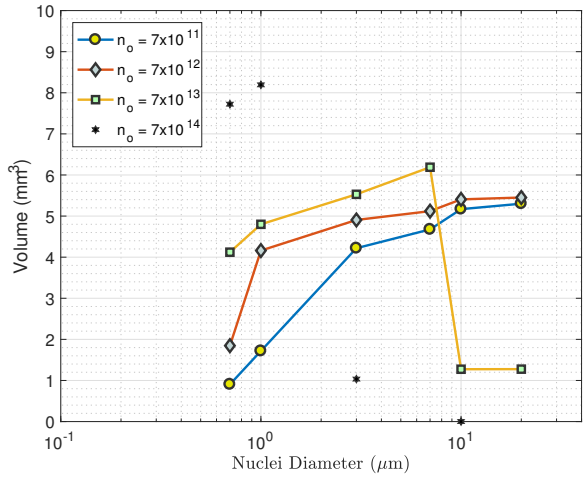

FIGURE 8. EFFECT OF NUCLEI SIZE AND CONCENTRATION ON VAPOR VOLUME PRODUCTION IN SCHNERR-SAUER CAVITATION MODEL

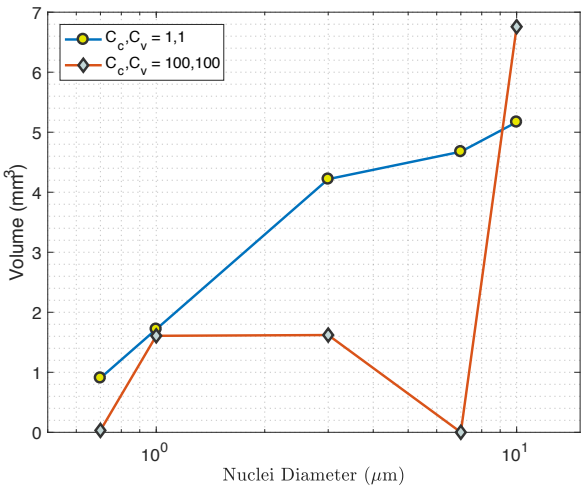

FIGURE 9. EFFECT OF EMPIRICAL CONSTANTS ON VAPOR VOLUME ON SCHNERR-SAUR MODEL

become markedly different if majority of the nozzle is initialized with a large amount of vapor as there are now two well defined phases. This differs from the physical experiments in which the volume of nuclei is very small compared to that of the liquid. Cazzoli et al. [29] makes mention of an upper limit of the d_{Nuc} specification. Current results define that nuclei diameter limit, and show that it decreases with increasing concentration of nuclei.

In addition to looking at the effects of nuclei size and concentration on vapor volume production, the constants of condensation and vaporization were also studied. For the Schnerr-Sauer model, they were both increased to take on values of 100. Figure 9 shows the comparison of vapor volume for a concentration of n_o = 7.0x10^{11} between constants of 1,1 and 100,100 for C_c and C_v respectively. It is found that increasing the rate resulted in significant reduction in the volume of vapor present at the end of the simulation.

As can be seen in the figure, less vapor volume is produced for all of the nuclei diameter investigated except the largest computed value of $10\mu m$. Moreover, the trend of increasing vapor volume with increases of nuclei diameter clearly seen in the constant case of 1,1, is not present for 100,100. The vapor volume plateaus after 1 μm and then a sharp decrease followed by an increase. The increase is inexplicable as the trend prior to that was not similar in nature at this bound. It is believed that the plateau seen after a diameter of $1\mu m$ is a similar artifact to the one seen in the 1,1 cases. There exists a threshold, in nuclei size for this case, after which the results become sporadic and unphysical. The increased rate constants move this threshold back to a smaller nuclei size of $1\mu m$ for this concentration. The remaining concentrations studied for the 100,100 case showed negligible amounts of vapor for all nuclei sizes. None of the studied parameter cases were able to provide proper qualitative comparisons between the simulations and the experiments. Nonetheless, key details on the sensitivity of the models to input parameter changes were ascertained.

Kunz Sensitivity

The Kunz cavitation model has only two free tuning parameters: C_c and C_v and two reference values U_∞ and t_∞ are required. In this work, the maximum velocity in the nozzle section of 48.59 m/s was specified. To define a reference time scale, the width of the nozzle was used to calculate a reference time using the aforementioned velocity. This value was calculated to be 0.000130 seconds. The various combinations used in this sensitivity analysis are outlined in table 4. The sensitivity analysis done here is similar to the one conducted on the Schnerr-Sauer model but there are now fewer parameters to change in order to determine if better agreement can be found. For all the simulations run using the Kunz model, the inlet velocity was set at 0.36 m/s, the largest inlet velocity, in hopes of producing the most vapor volume in the nozzle section.

TABLE 4. PARAMETERS USED IN SENSITIVITY STUDY FOR KUNZ MODEL

C_c	1	10	100	1000	1	100	100	1000
C_v	1	10	100	1000	100	1	1000	100

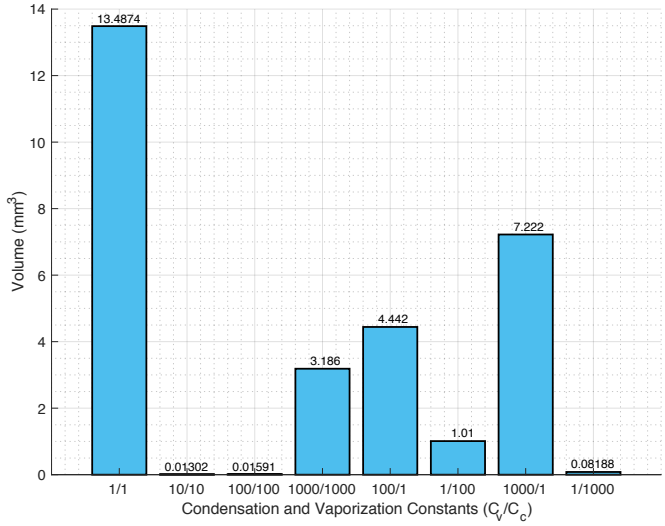

FIGURE 10. VAPOR PRODUCTION OF KUNZ MODEL FOR VARIOUS COMBINATIONS OF EMPIRICAL CONSTANTS

At the end of a simulation, an iso-volume of vapor was calculated for cells having vapor fractions of 0.5 or less. This allowed the vapor production to be quantified at the end of the simulation and related to the changes in empirical parameters. Figure 10 shows the changes in vapor volume with respect to changes in constants of condensation and vaporization. When C_c and C_v are 1, the simulation predicted the most vapor volume. Increasing both values to 10 and 100 produced negligible amounts of vapor while a further increase to a 1000 for both constants produced some vapor in the nozzle section. It is believed that since these constants control the rate of condensation and vaporization increasing the values results in exceedingly rapid production and destruction of vapor in the system. As such, the final vapor content is less than those with constants of smaller absolute value, however, the observation that 1000,1000 produces more vapor does not follow this logic.

When the ratio of C_v and C_c is larger than 1, vapor production is favored and indeed 1000/1 leads to more vapor than 100/1 and more than 1000/1000. While some trends are reasonable, the observation of 1/1 producing the most vapor volume remains an outlier. No combination of constants used in the Kunz cavitation model showed reasonable comparisons to the optical cavitation detection images obtained from the experiment. Figure 11 shows images of vapor volume fraction simulations obtained using the Kunz cavitation model. As can be seen the simulations severely under-predict the amount of cavitation seen in the experiments. A larger ratio between C_v and C_c could possibly produce a comparable image, nonetheless, the choice of the constants to obtain such an image is clearly heuristic.

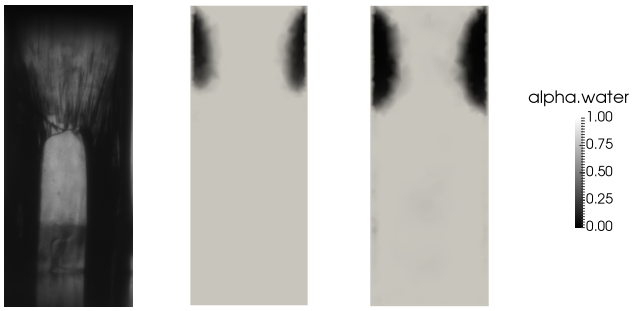

(a) Experiment (b) 1000/1 (c) 1/1

FIGURE 11. KUNZ MODEL SIMULATIONS

Model Comparison

While both models contain empirical parameters which require tuning to obtain cavitation levels which match experiment, the Schnerr-Sauer model seems to be a more natural choice to describe cavitation in nozzle flow. Having the ability to specify nuclei concentration and size is one of its main advantages. Nonetheless, given the nature of both models, being heavily dependent on empirical parameters, similar results can be obtained using both. Figure 12 shows the largest vapor volume observed using each model.

It can be seen that the Schnerr-Sauer images does a slightly better job at predicting the extent of the cavitating region. Both

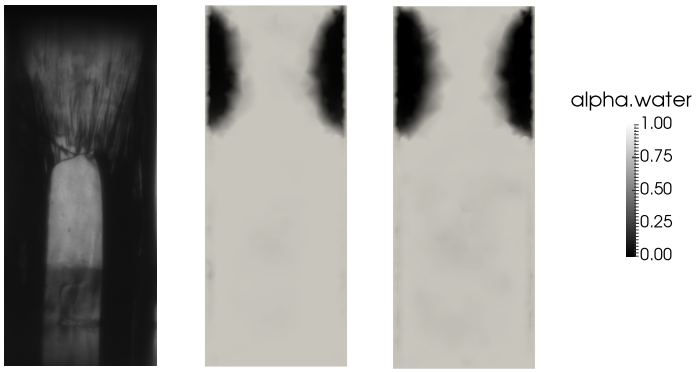

(a) Experiment (b) Kunz Model (c) Schnerr-Sauer Model

FIGURE 12. COMPARISON OF KUNZ AND SCHNERR-SAUER MODEL SIMULATIONS WITH EXPERIMENT

models however, for the parameters studied, were not able to yield comparable cavitation predictions as was seen in the experiments.

CONCLUSIONS

The current work presents an assessment of the cavitation models packaged in OpenFOAM in predicting cavitation in nozzle flow. The Kunz and Schnerr-Sauer cavitation models were studied. Both models have several free tuning parameters which affect cavitation predictions. Cavitation inception was studied. It was seen that the simulations, while able to correctly predict the measured velocities in the nozzle, severely underpredicted the amount of cavitation seen, and were able to properly discern a corresponding cavitation threshold, but unable to correctly predict the amount of vapor in the nozzle. This is partly due to the simplistic inception criterion employed in the Schnerr-Sauer model which simply compares local pressure in the domain to the saturated vapor pressure of the liquid, and the models' inability to specify a distribution of nuclei sizes.

For the Kunz model, constants C_c and C_v which control the rates of condensation and vaporization respectively must be specified. It was found that keeping the constants both at 1 resulted in the most vapor produced at the end of the simulations. Changing the constants such that one process was favored over the other provided reasonable results. A ratio for C_v/C_c of 1000/1 produced more vapor than that of 1/1000. Despite the heavily skewed preference for vaporization, keeping both constants at 1 resulted in the most vapor volume for the parameter sweep.

For the Schnerr-Sauer parameter model, the effects of empirical constants C_c, C_v, nuclei concentration, n_o and nuclei size, d_{Nuc} variations on cavitation prediction were studied. It was found that increasing nuclei size at a given concentration resulted in an increase in vapor volume, and similarly, increases in concentration for a given nuclei size also increases vapor volume. A threshold for vapor volume with increasing nuclei size was seen. Using larger nuclei sizes causes the volume of initial vapor to be of a similar order of magnitude as the computational domain. As such, the hydrodynamics of the system change and the simulated problem is no longer the same as those conducted in the experiments. An increase in the empirical constants from 1 to 100 produced less vapor than the previous case and plateaued at a smaller nuclei size.

Both models studied seemed to require a large amount of tuning to yield images which would be comparable to experimental results. While statements about the sensitivity of these models were ascertained, their development to provide accurate cavitation predictions is much needed. The inclusion of a more realistic inception criterion such as the Blake Threshold, and the specification of varying nuclei sizes in the fluid are key needed developments. Overall, the current work has assessed two popular cavitation models and discussed their limitations in predicting cavitation seen in nozzle flow.

Future work will be centered around investigating the outlier results via tighter parameter studies. Time averaged results will also be considered through a study of the pressure field and source term in the transport equation.

ACKNOWLEDGMENT

This material is based upon work supported by the Department of Energy, Office of Energy Efficiency and Renewable Energy (EERE) and the Department of Defense, Tank and Automotive Research, Development, and Engineering Center (TARDEC), under Award Number DEEE0007332.

REFERENCES

[1] Knapp, R. T., Daily, J. W., and Hammitt, F. G., 1970. *Cavitation*. McGraw Hill Book Company.

[2] Koukouvinis, P., Gavaises, M., Li, J., and Wang, L., 2016. "Large eddy simulation of diesel injector including cavitation effects and correlation to erosion damage". *Fuel,* ***175***, pp. 26–39.

[3] Mohammad Taghi Shervani-Tabar, Soran Parsa, M. G., 2012. "Numerical study on the effect of the cavitation phenomenon on the characteristics of fuel spray". *Mathematical and Computer Modelling,* ***56***, pp. 105–117.

[4] Changzhao Jiang, Hongming Xu, D. S. X. M. K. D. R. C. J. K.-V., 2017. "Effect of fuel injector deposit on spray characteristics, gaseous emissions and particular matter in a gasoline direct injection engine". *Applied Energy,* ***203***, pp. 390–402.

[5] Salvador, F. J., Romero, J. V., Rosello, M. D., and Martinez-Lopez, J., 2010. "Validation of a code for modeling cavitation phenomena in diesel injector nozzles". *Mathematical and Computer Modelling,* ***52***, pp. 1123–1132.

[6] Tahmasebi, E., Lucchini, T., D'Errico, G., and Onorati, A., 2015. "Numerical simulation of diesel injector internal flow field". In 70th Conference of the ATI Engineering Association, E. Procedia, ed., Vol. 82, pp. 51–58.

[7] Payri, R., Margot, X., and Salvador, F. J., 2002. "A numerical study of the influence of diesel nozzle geometry on the inner cavitating flow". In Society of Automotive Engineers.

[8] Bicer, B., and Sou, A., 2015. "Application of the improved cavitation model to turbulent cavitating flow in fuel injector nozzle". *Applied Mathematical Modelling,* ***40***, November, pp. 4712–4726.

[9] Ahuja, V., Hosangadi, A., and Arunajatesan, S., 2001. "Simulation of cavitating flows using hybrid unstructured meshes". *Journal of Fluids Engineering,* ***123***, pp. 331–339.

[10] Yu, H., Goldsworthy, L., Brandner, P. A., and Garaniya, V., 2017. "Development of a compressible multiphase cavita-

tion approach for diesel spray modelling". *Applied Mathematical Modelling,* ***45***(705-727).

[11] Srinivasan, V., Salazar, A. J., and Saito, K., 2009. "Numerical simulation of cavitation dynamics using a cavitation-induced-momentum-defect (cimd) correction approach". *Applied Mathematical Modelling,* ***33***, pp. 1529–1559.

[12] Singhal, A. K., Athavale, M. M., Li, H., and Yu, J., 2002. "Mathematical basis and validation of the full cavitation model". *Transactions of ASME, Journal of Fluid Engineering,* ***124***, pp. 617–624.

[13] Zhao, H., Quan, S., Dai, M., Pomraning, E., Senecal, P. K., Xue, Q., Battistoni, M., and Som, S., 2014. "Validation of a three-dimensional internal nozzle flow model including automatic mesh generation and cavitation effects". *Journal of Engineering for Gas Turbines and Power*.

[14] Desantes, J., Garcia-Oliver, J. M., Pastor, J. M., Pandal, A., Baldwin, E., and Schmidt, D. P., 2016. "Coupled/decoupled spray simulation of the ecn spray: A condition with the sigma-y eulerian atomization model". *International Journal of Multiphase Flow,* ***80***, pp. 89–99.

[15] Duke, D. J., Schmidt, D. P., Neroorkarand, K. D., Kastengren, A. L., and Powell, C. F., 2013. "High resolution large eddy simulations of cavitating gasoline-ethanol blends". *International Journal of Engine Research*.

[16] la Morena, J. D., Neroorkar, K. D., Plazas, A. H., Peterson, R. C., and Schmidt, D. P., 2013. "Numerical analysis of the influence of diesel nozzle design on the internal flow characteristics of tilted injectors". *Atomization and Sprays,* ***23***(2), pp. 97–118.

[17] Neroorkar, K. D., II, C. E. M., Plazas, A. H., Grover, R. O., and Schmidt, D. P., 2012. "Simulations and analysis of fuel flow in an injector including transient neddle effects". In ILASS-Americas 24th Annual Conference on Liquid Atomization and Spray Systems, San Antonio TX.

[18] Schmidt, D. P., Rutland, C. J., and Corradini, M. L., 1999. "A fully compressible, two-dimensional model of small, high-speed, cavitating nozzles". *Atomization and Sprays,* ***9***, pp. 255–276.

[19] Trask, N., Schmidt, D. P., Lightfoot, M. D. A., and Danczyk, S. A., 2012. "Compressible modeling of the internal two-phase flow in a gas-centered swirl coaxial fuel injector". *Journal of Propulsion and Power,* ***28***(4), pp. 685–693.

[20] Goplan, S., and Katz, J., 2000. "Flow structure and modeling issues in the closure region of attached cavitation". *Physics of Fluids,* ***12***(4), pp. 895–911.

[21] Ducoin, A., Huang, B., and Young, Y. L., 2012. "Numerical modeling of unsteady cavitating flows around a stationary hydrofoil". *International Journal of Rotating Machinery*.

[22] Kunz, R. F., Boger, D. A., Stinebring, D. R., Chyczewski, T. S., Lindau, J. W., Gibeling, H. J., Venkateswaran, S., and Govindan, T. R., 2000. "A preconditioned navier-stokes method for two-phase flows with application to cavitation prediction". *Computers and Fluids,* ***29***, pp. 849–875.

[23] Merkle, C. L., Feng, J., and Buelow, P. E., 1998. "Computational modeling of the dynamics of sheet cavitation". In 3rd International Symposium on Cavitation, Grenoble, France, Vol. 2, pp. 47–54.

[24] Sauer, J., and Schnerr, G. H., 2000. "Unsteady cavitating flow - a new cavitation model based on a modified front capturing method and bubble dynamics". In Proceedings of FEDSM'00 (ASME Fluids Engineering Summer Conference).

[25] OpenFOAM, 2016. *OpenFOAM User Guide*. CFD Direct, September.

[26] Bicer, B., 2016. "Numerical simulation of cavitation phenomena inside fuel injector nozzles". PhD thesis, Kobe University, September.

[27] Holland, C. K., and Apfel, R. E., 1989. "An improved theory for the prediction of microcavitation thresholds". *IEE Transactions on Ultrasonics, Ferroelectrics and Frequency Control,* ***36***(2), pp. 204–208.

[28] Dabiri, S., Sirignano, W. A., and Joseph, D. D., 2007. "Cavitation in an orifice flow". *Physics of Fluids,* ***19***(072112).

[29] GiulioCazzoli, Falfari, S., Bianchi, G., Forte, C., and Catellani, C., 2016. "Assessment of the cavitation models implemented in openfoam under di-like conditions". In 71st Conference of the Italian Thermal Machines Engineering Association, E. Procedia, ed., Vol. 101, pp. 638–645.